

# From Complex Chains to 1D Metal Oxides: A Novel Strategy to Cu<sub>2</sub>O Nanowires

Yujie Xiong, Zhengquan Li, Rong Zhang, Yi Xie,\* Jun Yang, and Changzheng Wu

Structure Research Laboratory, Department of Chemistry, University of Science and Technology of China, Hefei, Anhui 230026, P. R. China

Received: September 26, 2002; In Final Form: December 23, 2002

A new strategy has been put forward that small complexes with several linear-aligned metal cations can provide precursors for the growth of metal oxide nanowires, if they can be linearly connected with each other by bridging anions with rodlike micelles confined. As an example, Cu<sub>2</sub>O monocrystalline nanowires were prepared via a novel complex-precursor surfactant-assisted (CPSA) route, in which linear alignment of copper cations in Cu<sub>3</sub>(dmg)<sub>2</sub>Cl<sub>4</sub> as precursors provided orientation for the growth of Cu<sub>2</sub>O nanowires while rodlike SDS micelles drove the linear units of Cu<sub>3</sub>(dmg)<sub>2</sub>Cl<sub>4</sub> to connect with each other by Cl anions to form [Cu<sub>3</sub>(dmg)<sub>2</sub>Cl<sub>2</sub>]<sub>n</sub><sup>2n+</sup> and confined the diameter of nanowires. The infrared absorption spectra and laser light scattering show our strategy is reasonable and successful. The band gap of Cu<sub>2</sub>O nanowires was determined to 2.34 eV by UV–vis absorption spectrum, showing its promising application for the reversible conversion between solar energy and electrical or chemical energy. This method can be easily controlled and is expected to extend to fabricate other metal oxide or chalcogenide 1D nanomaterials.

## Introduction

Controlling the shape of nanostructures at the mesoscopic level is one of the most challenging issues presently faced by synthetic inorganic chemists.<sup>1</sup> Especially, in the past few years, nanowires, which are one-dimensional (1D) objects, have attracted particular attention, because of their unusual properties and potential utilization in electric, magnetic, optical, and micromechanical devices.<sup>2–8</sup> However, the fabrication or synthesis of these 1D materials is a challenge owing to their extremely small size and their anisotropy. The control of nucleation and growth of 1D nanostructural materials is becoming critical. Many methods have been used to prepare nanowires, such as electrochemistry,<sup>2</sup> template (mesoporous silica, carbon nanotubes, etc.),<sup>3</sup> emulsion or polymeric system,<sup>4</sup> laser-assisted catalysis growth,<sup>5</sup> solution,<sup>6</sup> vapor transport,<sup>7</sup> and organometallic and coordination chemistry methods.<sup>8</sup> Among these methods, the lattermost one, avoiding complicated processes and special instruments, can be extended to prepare metal or metal oxide nanowires. Most remarkably, this method gives more attention to the relationship between structure and morphology of as-desired materials.

In particular, metal oxide nanowires are of interest, because of both their fundamental importance and the wide range of their potential applications in nanodevices. Semiconducting, one-dimensional, nanosized materials are known to have many interesting physical properties and great applications in optoelectronic devices, such as nanowire light-emitting devices with extremely low power consumption. For example, cuprous oxide and related materials are the subject of much current interest. Cu<sub>2</sub>O is a p-type semiconductor with a direct band gap of 2 eV, and excitons can propagate coherently through its monocrystalline samples,<sup>9</sup> which make it a promising material for the reversible conversion between solar energy and electrical or chemical energy. Cu/Cu<sub>2</sub>O layered nanostructured materials

with interesting optoelectronic properties have been prepared by electrodeposition.<sup>10</sup> Another exciting development is a Cu<sub>2</sub>O related material, CuAlO<sub>2</sub>, that was reported as the first transparent oxide showing appreciable p-type conductivity (up to 1 S/cm).<sup>11</sup> Recently, it has been found that Cu<sub>2</sub>O submicrospheres can be used as the negative electrode material for lithium ion batteries.<sup>12</sup> The previous research shows that 1D systems, as the smallest dimension structures for efficient transport of electrons, could be applied to detect the theoretical operating limits of Lithium batteries,<sup>13</sup> indicating more applications of Cu<sub>2</sub>O nanowires.

In this work, Cu<sub>2</sub>O monocrystalline nanowires were prepared via a novel complex-precursor surfactant-assisted (CPSA) route, in which linear alignment of copper cations in Cu<sub>3</sub>(dmg)<sub>2</sub>Cl<sub>4</sub> as precursors provided orientation for the growth of Cu<sub>2</sub>O nanowires while rodlike SDS micelles drove the units of Cu<sub>3</sub>(dmg)<sub>2</sub>Cl<sub>4</sub> to connect with each other by Cl anions to form [Cu<sub>3</sub>(dmg)<sub>2</sub>Cl<sub>2</sub>]<sub>n</sub><sup>2n+</sup> and confined the diameter of nanowires.

## Experimental Sections

Details of the experimental process can be described as following. First, the Cu(dmg)<sub>2</sub> was prepared by adding 2 mmol Cu(Ac)<sub>2</sub>·2H<sub>2</sub>O to a solution of 4 mmol dmgH in 50 mL of ethanol. Then 4 mmol CuCl<sub>2</sub>·2H<sub>2</sub>O was dissolved in 15 mL ethanol and was added dropwise to 2 mmol Cu(dmg)<sub>2</sub> in 50 mL ethanol and continuously stirred. The brownish green crystals of Cu<sub>3</sub>(dmg)<sub>2</sub>Cl<sub>4</sub> were collected after 12 h<sup>14</sup> and then were dissolved in 10 mL of distilled water to make solution A by ultrasonic disperse for the posterior reactions. Then the mixture of solution A, 30 mL of cyclohexane, 1.25 g of SDS, 1.5 mL pf 1-octanol, and 2 mL of glucose solution (0.400 g of glucose was dissolved and diluted to 50 mL with H<sub>2</sub>O), was loaded into a 50-mL Teflon-lined autoclave, which was then filled with cyclohexane up to 90% of the total volume. (The concentration (102 mmol/L) of surfactant is above nine times the critical micelle concentration (11 mmol/L).<sup>14</sup>) The autoclave was sealed, warmed at 1 °C/min, and maintained at 60 °C for

\* To whom correspondence should be addressed. E-mail: yxielab@ustc.edu.cn. Fax: 86-551-3603987. Phone: 86-551-3603987.

4 h and was then cooled to room-temperature naturally. The precipitate was filtered off, washed with distilled water and absolute ethanol for several times, and then dried in a vacuum at 60 °C for 4 h.

X-ray diffraction (XRD) patterns were carried out on a Japan Rigaku D/max rA X-ray diffractometer equipped with graphite monochromatized high-intensity Cu K $\alpha$  radiation ( $\lambda = 1.54178$  Å). The X-ray photoelectron spectra (XPS) were collected on an ESCALab MKII X-ray photoelectron spectrometer, using nonmonochromatized Mg K $\alpha$  X-ray as the excitation source. Field emission scanning electron microscopy (FE-SEM) images were taken on a JEOL JSM-6700F SEM. Transmission electron microscopy (TEM) images and electronic diffraction (ED) patterns were taken on a Hitachi model H-800 instrument with a tungsten filament, using an accelerating voltage of 200 kV. High-resolution transmission electron microscopy (HRTEM) images were performed with a JEOL-2010 TEM at an acceleration voltage of 200 KV. Infrared absorption (IR) spectra were performed with a Nicolet FT-IR-170SX spectrometer in the range of 150–300 and 1000–4000 cm<sup>-1</sup> at room temperature, with the sample in a KBr disk or cell. Ultraviolet and visible light (UV–vis) spectra were recorded on a JGNA Specord 200 PC UV–vis spectrophotometer.

As for the characterization of laser light scattering, a commercial laser light scattering spectrometer (ALV/SP-150) equipped with a solid-state laser (ADLAS DPY425II, output power 400 mW at  $\lambda = 532$  nm) as the light source and an ALV-5000 multi- $\tau$  digital correlator were used. The samples were filtered through a 0.5 mm Millipore filter into the cylindrical light scattering cell. The specific refractive index increment ( $dn/dc$ ) used in static light scattering was determined by a novel and precise differential refractometer.

## Results and Discussion

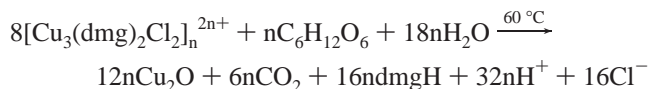
**General Strategy for Metal Oxide Nanowires.** In the field of coordination chemistry, many complexes have stable infinite ordered structures, because of the rigidity of bridging ligands. In particular, metal cations in some complexes arrange on long chains, bridged by certain ligands. These long chains might provide orientation for the growth of metal or metal oxide nanowires via suitable reactions. However, the complexes with infinite structures are usually stable and their ligands are difficult to leave from metal cations. Thus, the transformation from these complexes to metal or metal oxide is not convenient. Moreover, the preparation of these complexes need complicated procedures and long time, limiting their applications in synthesizing metal or metal oxide nanowires. On the other hand, the formation of small units with several linear-aligned metal cations is very common in the complexes of transition metals, the preparation of these small complexes is considerably convenient and their ligands are easy to leave from metal cations, but the key problem is how to drive them to connect with each other to form longer chains. Some bridging anions, such as halogen ions, can connect the units to lengthen the linear chains containing metal cations. However, under disorder reaction condition, the bridging effect is limited. The previous colloidal research shows that the rodlike micelle can offer a unique microenvironment for chemical reactions and reduce the systematic disorder to small area. It should be an excellent candidate for driving the small linear units' connecting action by bridging anions. Thus, the long chains bridged by bridging anions in rodlike micelles can provide orientation for the growth of metal oxide nanowires via suitable reactions.

**The Special Case in This Work.** From the above strategy, the first problem to solve is selecting a complex-precursor with

several linear-aligned copper cations. It is well-known that Cu<sup>2+</sup> can be combined with N and O atoms of dimethylglyoxime (dmgH), forming the trinuclear complex of Cu<sub>3</sub>(dmg)<sub>2</sub>Cl<sub>4</sub>,<sup>15</sup> in which every 3 copper cations compose of a unit and arrange on a line (Scheme 1A). The units composed of three copper cations on lines can be bridged by Cl anions, resulting in the formation of longer chains containing copper cations. It is thought that if the copper(II) cations on chains in the complex may be reduced by glucose to produce Cu<sub>2</sub>O, the complex can be used as precursor, in which the 1D array of copper cations will provide orientation for the growth of Cu<sub>2</sub>O nanowires.

However, the bridging effect of Cl anions is too limited to connect copper cations of every unit to form enough long chains. To solve this problem, an efficient way is to build up rodlike micelles composed of surfactant to confine the linear units of Cu<sub>3</sub>(dmg)<sub>2</sub>Cl<sub>4</sub> in microenvironments and reduce the systematic disorder, in which the Cu<sub>3</sub>(dmg)<sub>2</sub>Cl<sub>4</sub> units are driven to connect with each other by Cl anions to form [Cu<sub>3</sub>(dmg)<sub>2</sub>Cl<sub>2</sub>]<sub>n</sub><sup>2n+</sup> (as shown in Scheme 1B), in which the remain Cl<sup>-</sup> anions are dissociated near and remain the electric neutrality of reaction system. The rodlike micelles are both hydrophobic and hydrophilic (W/O), forming when the concentration of surfactant is as 10 times as critical micelle concentration.<sup>14</sup> It is obvious that the complex-precursor forms in water phase, enwrapped in rodlike micelles. Thus, the copper cations in the complex can arrange on long chains of [Cu<sub>3</sub>(dmg)<sub>2</sub>Cl<sub>2</sub>]<sub>n</sub><sup>2n+</sup> in the rodlike micelles and provide orientation for the growth of Cu<sub>2</sub>O nanowires, when the copper(II) cations in the complex are reduced to Cu<sub>2</sub>O by glucose. Further studies indicate that the rodlike micelles cannot only drive linear units of Cu<sub>3</sub>(dmg)<sub>2</sub>Cl<sub>4</sub> to connect with each other but also confine the diameter of nanowires.

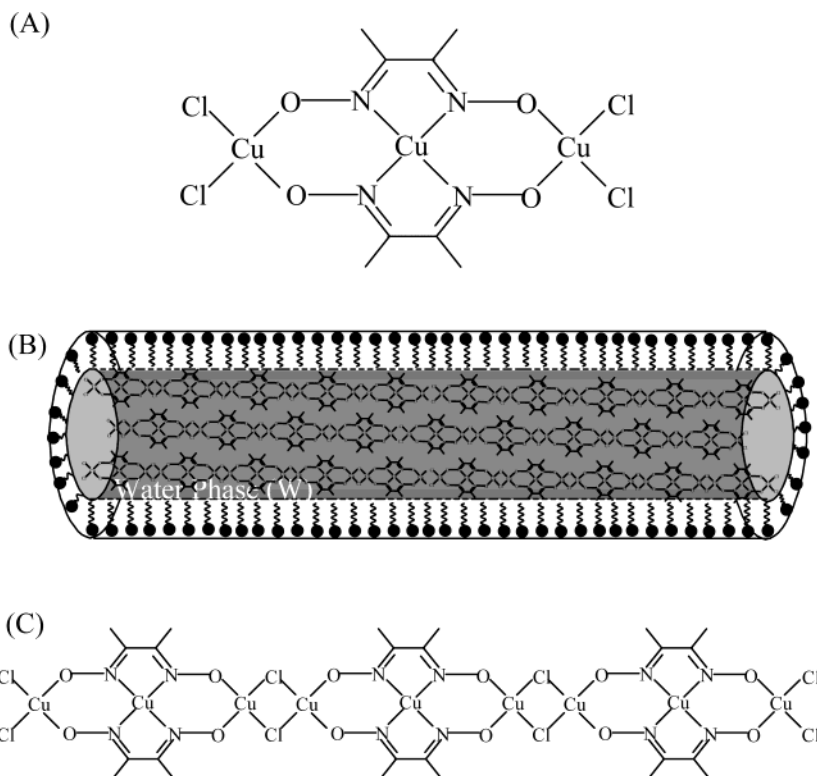
**Synthesis Route.** On the basis of the above strategy, a novel complex-precursor surfactant-assisted (CPSA) route was designed to prepare Cu<sub>2</sub>O monocrystalline nanowires: [Cu<sub>3</sub>(dmg)<sub>2</sub>Cl<sub>2</sub>]<sub>n</sub><sup>2n+</sup> was first prepared in SDS micelles at room temperature, which was then reduced into Cu<sub>2</sub>O nanowires by glucose at 60 °C



**Phase and Purity of As-Obtained Products.** The phase and purity of as-prepared products were determined by the X-ray diffraction (XRD) patterns, shown in Figure 1A. All of the reflection peaks can be indexed to cubic Cu<sub>2</sub>O (JCPDS Card Files, 5-667) with the lattice parameter  $a = 4.2696$  Å. No characteristic peaks were observed for the other impurities such as Cu or CuO.

Important information about the surface molecular and electronic structure of the Cu<sub>2</sub>O nanowires was provided by X-ray photoelectron spectra (XPS). The binding energies obtained in the XPS analysis were corrected for specimen charging by referencing the C1s to 284.60 eV. The Cu 2p core level spectrum (Figure 2A) illustrates that the observed value of the binding energies for Cu 2p<sub>3/2</sub> and Cu 2p<sub>1/2</sub> are in agreement with the literature values of bulk for Cu<sup>+</sup>.<sup>16</sup> Besides, the Cu 2p<sub>3/2</sub> satellite peaks characterizing Cu<sup>2+</sup>, which are usually centered at about 942 eV,<sup>17</sup> are not found in Figure 2A. The O 1s binding energies (Figure 2B) of the  $\gamma$ -MnO<sub>2</sub> nanowires, 529.2 eV, can be thought as the O (-2) in the compounds.<sup>18</sup> The weaker shoulder peak at ~532.0 eV in the spectra of  $\gamma$ -MnO<sub>2</sub> nanowires is ascribed to the O from absorbed gaseous molecules. All of these results indicate that the samples

**SCHEME 1:** (A) Structure of Trinuclear Complex Cu<sub>3</sub>(dmg)<sub>2</sub>Cl<sub>4</sub> and (B) Arrangement of Cu<sub>3</sub>(dmg)<sub>2</sub>Cl<sub>4</sub> Connected by Cl Anions to Form [Cu<sub>3</sub>(dmg)<sub>2</sub>Cl<sub>2</sub>]<sub>n</sub><sup>2n+</sup> in SDS Micelles, while the Remaining Chlorides Are Dissociated near and Remain the Electric Neutrality of Reaction System<sup>a</sup>



<sup>a</sup> Considering the Schematic Space, the Drawing Cannot Describe the Size Ratio of Micelle to Chain Containing Copper Cations and Only Three Chains Are Shown in This Micelle. (•••••): SDS (C) Structural Details for a [Cu<sub>3</sub>(dmg)<sub>2</sub>Cl<sub>2</sub>]<sub>n</sub><sup>2n+</sup> Chain in SDS.

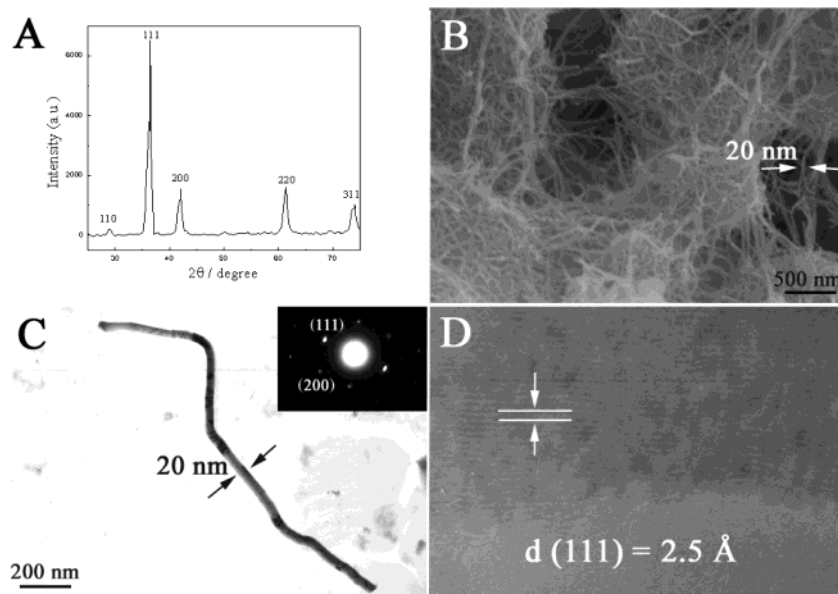


**Figure 1.** (A) XRD pattern of as-obtained Cu<sub>2</sub>O nanowires. (B) FE-SEM image of as-obtained Cu<sub>2</sub>O nanowires. (C) TEM image of a Cu<sub>2</sub>O nanowire (inset is its ED pattern). (D) HRTEM image of a Cu<sub>2</sub>O nanowire.

are Cu<sub>2</sub>O, and the XPS survey spectra show that no obvious impurities could be detected in the samples, indicating that the level of impurities is lower than the resolution limit of XPS (1 at.%).

**Some Experiments and Characterizations to Confirm Mechanism.** *Characterization of Cu<sub>3</sub>(dmg)<sub>2</sub>Cl<sub>4</sub>.* The Cu<sub>3</sub>(dmg)<sub>2</sub>Cl<sub>4</sub> was characterized by elemental analysis and infrared absorption (IR) spectrum. The elemental analytical results (Table 1) show the composition of Cu<sub>3</sub>(dmg)<sub>2</sub>Cl<sub>4</sub>, which is close to

the calculated and literature data.<sup>14</sup> In the IR spectrum (Figure 3) of the complex, the absorption peaks at 1515 and 1200, 1065 cm<sup>-1</sup> are indexed to the C=N and N-O bands, with some shifts to a low-frequency region as compared to Cu(dmg)<sub>2</sub>.<sup>14</sup> O-H appears at a higher frequency region as compared to dmgH. All these results are in agreement with the literature for Cu<sub>3</sub>(dmg)<sub>2</sub>Cl<sub>4</sub>,<sup>14</sup> revealing the trinuclear structure of precursor.

*Far-IR Spectra.* To investigate the effect of SDS micelles on the small linear units in the complex, the far-infrared

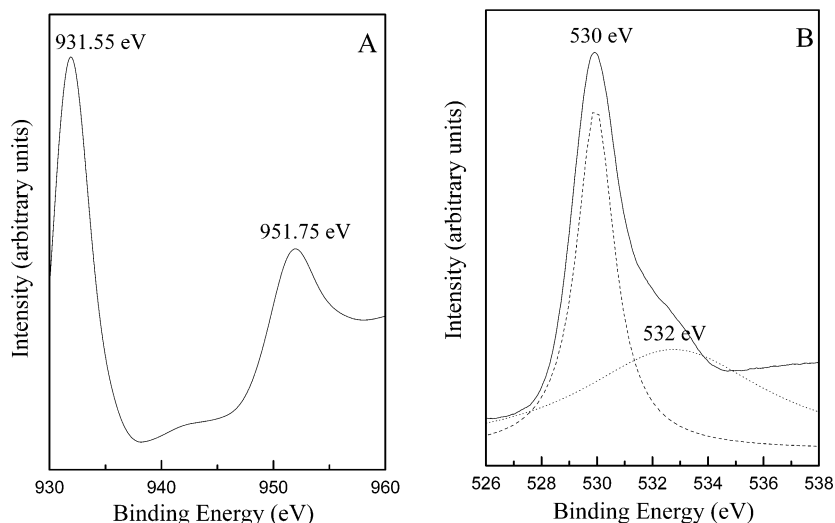


**Figure 2.** (A) Cu 2p core level spectrum of Cu<sub>2</sub>O nanowires. (B) O 1s core level spectrum of Cu<sub>2</sub>O nanowires.

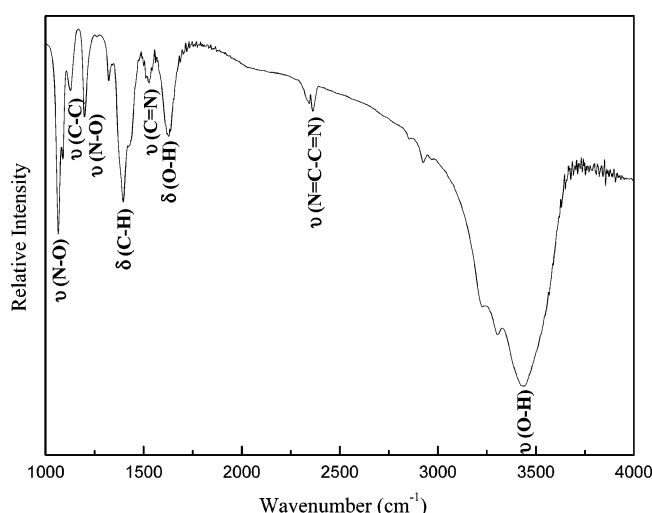


**Figure 3.** IR spectrum of Cu<sub>3</sub>(dmgl)<sub>2</sub>Cl<sub>4</sub> crystals.

**TABLE 1: Elemental Analytical Results for Cu<sub>3</sub>(dmgl)<sub>2</sub>Cl<sub>4</sub>**

	copper %	chlorine %	carbon %	hydrogen %	nitrogen %
expt	33.48	25.27	17.44	3.01	9.92
lit	33.29	25.20	17.89	3.04	9.90
calcd	33.69	25.31	17.05	2.50	10.00

absorption (IR) spectra were provided. The solution containing Cu<sub>3</sub>(dmgl)<sub>2</sub>Cl<sub>4</sub> without adding SDS was determined by the IR spectrum (Figure 4A); in the far-IR region, the absorption peaks at 201–204, 251, and 226, 282 cm<sup>-1</sup> were Cu–Cl stretching vibration,<sup>19</sup> Cu–O stretching vibration,<sup>20</sup> and Cu–N stretching vibration,<sup>20</sup> respectively, whereas the absorption peaks corresponding to Cu–Cl–Cu stretching vibration<sup>19</sup> (170–174 cm<sup>-1</sup>) were not clearly seen in the spectrum (terminal: bridging = 7:1). It shows that few of the Cl anions in the complex act as bridge atoms without adding SDS to solution. By comparison, with adding SDS, the solution containing micelles and complexes was then determined by IR spectra. It was found from the IR spectrum (Figure 4B) that the absorption peaks of Cu–O stretching vibration and Cu–N stretching vibration remained and those of Cu–Cl stretching vibration were weakened a lot, whereas that of Cu–Cl–Cu stretching vibration appeared (terminal: bridging = 1:10). To investigate whether the complexes are in micelles or outside, the clarified solution after maintaining for a long time was measure by the far-IR spectrum. No absorption peak was found in the IR spectrum of clarified

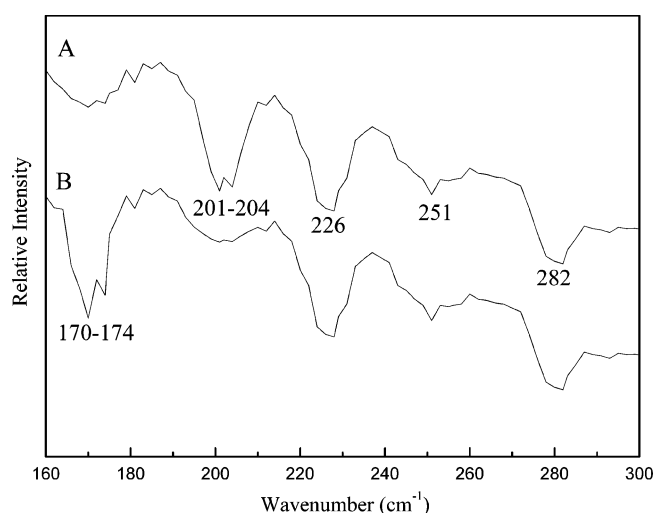


**Figure 4.** Far-IR spectra of (A) the solution containing Cu<sub>3</sub>(dmgl)<sub>2</sub>Cl<sub>4</sub> without adding SDS. (B) the solution containing [Cu<sub>3</sub>(dmgl)<sub>2</sub>Cl<sub>4</sub>]<sub>n</sub><sup>2n+</sup> with adding SDS.

solution. These results indicate the linear units of Cu<sub>3</sub>(dmgl)<sub>2</sub>Cl<sub>4</sub> form longer chains in [Cu<sub>3</sub>(dmgl)<sub>2</sub>Cl<sub>4</sub>]<sub>n</sub><sup>2n+</sup> by the bridge of Cl anions, enwrapped in rodlike SDS micelles.

**LLS.** To confirm the aggregation type of micelles, it was determined by the laser light scattering (LLS).

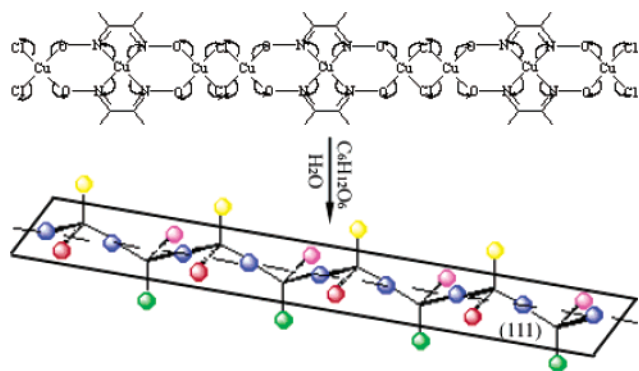
In static LLS, the angular dependence of the absolute excess time-average scattered intensity, know as the Rayleigh ratio  $R_{vv}(q)$ , is related to the weight-average molar mass ( $M_w$ ), the z-average root-mean-square radius of gyration ( $\langle R_g^2 \rangle_z^{1/2}$  or written as  $\langle R_g \rangle$ ) and the second virial coefficient ( $A_2$ ) of the scattering objects

$$\frac{KC}{R_{vv}(q)} \cong \frac{1}{M_w} \left( 1 + \frac{1}{3} \langle R_g^2 \rangle_z q^2 \right) + 2A_2C$$

where  $q = (4\pi n/\lambda) \sin(\theta/2)$  with  $n$ ,  $\lambda$ , and  $\theta$  being the refractive index of solvent, the wavelength of the light in a vacuum, and the scattering angle, respectively. In dynamic LLS, the cumulant or Laplace inversion analysis of the measured intensity–intensity time correlation function  $G^{(2)}(q, t)$  in the self-beating mode can lead to an average line width ( $\langle \Gamma \rangle$ ) or a line width distribution ( $G(\Gamma)$ ).<sup>21,22</sup> For a pure diffusion coefficient  $D$  via  $\Gamma = Dq^2$  at  $C \rightarrow 0$  and  $q \rightarrow 0$ ,<sup>23</sup> or the hydrodynamic radius ( $R_h$ ) by the Stokes–Einstein equation,  $D = k_B T / (6\pi\eta R_h)$ , where



**SCHEME 2: Reaction Process of  $[\text{Cu}_3(\text{dmg})_2\text{Cl}_2]_n^{2n+}$  Reduced by Glucose to Form Cu<sub>2</sub>O in Micelles<sup>a</sup>**



<sup>a</sup> The Dots of Each Color Represent the Copper Atoms on a Line Connected by Oxygen Atoms. The Blue, Red, and Purple Dots Are on a (111) Plane, whereas the Yellow and Green Dots Are on Other Planes of {111}.

$k_B$ ,  $T$ , and  $\eta$  are the Boltzman constant, the absolute temperature, and the solvent viscosity, respectively.

The parameters of  $dn/dc$ ,  $R_g$ ,  $R_h$ , and  $M_w$  were determined to be 0.155, 42.10, and 20.09 nm and  $6.3 \times 10^5$ . The rate of  $R_g/R_h$  is 0.775 for spheres and 2 for rigid rods according to theoretical prediction.<sup>24</sup> Here, both  $R_g$  and  $R_h$  are above 20 nm and  $R_g/R_h$  is about 2, suggesting the micelles are rodlike.

**Other Experiments.** The supplementary experiments were also carried out to confirm the formation mechanism of Cu<sub>2</sub>O nanowires. Without adding dmgH to form complex, no nanowire could be obtained. When no SDS micelles built up, only some short needlelike nanocrystals were obtained. It further confirms that both complex-precursor and SDS micelles are crucial to the formation of Cu<sub>2</sub>O nanowires.

These results confirm that the selecting of complex-precursor is successful and our strategy that the rodlike micelles can drive linear units of  $\text{Cu}_3(\text{dmg})_2\text{Cl}_4$  to connect with each other is reasonable.

**The Morphology and Growth Direction of As-Obtained Products.** The panoramic morphologies of as-obtained products were examined by the field emission scanning electron microscopy (FE-SEM), which the solid samples were mounted on a copper mesh without any dispersion treatment, indicating that all samples (Figure 1B) are uniform nanowires, the diameters of nanowires are ca. 20 nm and the lengths range from 3 to 6  $\mu\text{m}$ . The diameter of nanowires is in agreement with that of rodlike micelles (usually  $\sim 20$  nm), revealing that the nanowires should grow in the micelles. Figure 1C shows the transmission electron microscopy (TEM) image of several such nanowires, indicating the uniformity in diameter along each wire.

The more details about the structure of nanowires were investigated by the electronic diffraction (ED) and high-resolution transmission electron microscopy (HRTEM). The HRTEM image (Figure 1D) of nanowires shows that the as-obtained nanowires are structurally uniform and the grow plane of nanowires is one of the {111} planes of cubic Cu<sub>2</sub>O, indicating the rationality of our strategy that Cu<sub>2</sub>O nanowires orientated-grow along chains containing copper cations. The ED pattern (inset in Figure 1C) further confirms that the as-obtained product is monocrystalline.

**Formation Mechanism of Cu<sub>2</sub>O Nanowires.** As described in the above strategy section, the  $[\text{Cu}_3(\text{dmg})_2\text{Cl}_2]_n^{2n+}$  chains provide a direction for the 1D oriented growth of nanowires. From the HRTEM and ED observation, the Cu<sub>2</sub>O nanowires grow along (111) plane. From its structural characteristics, one

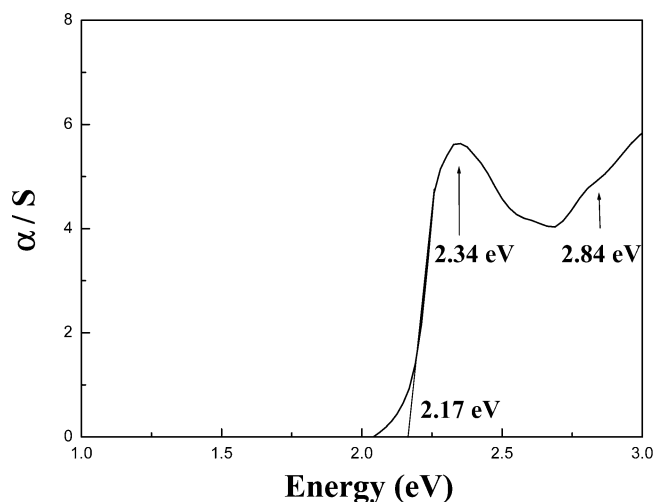


**Figure 5.** UV-vis spectrum of as-prepared Cu<sub>2</sub>O nanowires.

can see that Cu<sub>2</sub>O consists of some parallel chains containing copper atoms on (111) plane, which are connected with each other by oxygen atoms. It is proposed that the  $[\text{Cu}_3(\text{dmg})_2\text{Cl}_2]_n^{2n+}$  chains actually provide a direction for the formation of chains in (111) plane of Cu<sub>2</sub>O, thus resulting in the (111) oriented growth of Cu<sub>2</sub>O nanowires via reduction reactions (Scheme 2). During the process of reduction, all of the chains in the same rodlike micelles will connect with each other by forming new Cu–O bonds of Cu<sub>2</sub>O, resulting in the other 2D growth. Obviously, the reaction carries out in the rodlike micelles and the diameter of nanowires is confined by the micelles. As a matter of fact, the diameter of nanowires is in agreement with that of rodlike micelles ( $\sim 20$  nm).

**Optical Property of As-Obtained Products.** The optical property of Cu<sub>2</sub>O nanowires was investigated with room-temperature ultraviolet and visible light (UV-vis) absorption spectroscopy (Figure 5). The Cu<sub>2</sub>O nanowires possess well defined, sharp optical absorption associated with band gap transition at 2.34 eV. The very sharp electronic transition suggests that its band gap may possibly direct. Comparing with the direct band gap (2 eV) of bulk Cu<sub>2</sub>O, there exists obvious blue shift between them, indicating the strong quantum confinement of the excitonic transition expected for Cu<sub>2</sub>O nanowires. This band gap of 2.34 eV makes it a more promising material for the reversible conversion between solar energy and electrical or chemical energy.

## Conclusions

In summary, a new strategy has been put forward that small complexes with several linear-aligned metal cations can provide precursors for the growth of metal oxide nanowires, if they can be linearly connected with each other by bridging anions with rodlike micelles confined. As an example, Cu<sub>2</sub>O monocrystalline nanowires were prepared via a novel complex-precursor surfactant-assisted (CPSA) route, in which linear alignment of copper cations in  $\text{Cu}_3(\text{dmg})_2\text{Cl}_4$  as precursors provided orientation for the growth of Cu<sub>2</sub>O nanowires while rodlike SDS micelles drove the linear units of  $\text{Cu}_3(\text{dmg})_2\text{Cl}_4$  to connect with each other by Cl anions to form  $[\text{Cu}_3(\text{dmg})_2\text{Cl}_2]_n^{2n+}$  and confined the diameter of nanowires. The infrared absorption spectra (IR) and laser light scattering (LLS) show our strategy is reasonable and successful. The band gap of Cu<sub>2</sub>O nanowires was determined to 2.34 eV by UV-vis absorption spectrum, showing its promising application for the reversible conversion between solar energy and electrical or chemical energy. This

method can be easily controlled and is expected to extend to fabricate other metal oxide or chalcogenide 1D nanomaterials.

**Acknowledgment.** This work was supported by the National Natural Science Foundation of China and Chinese Ministry of Education. The authors thank Prof. Shuyuan Zhang, Prof. Chi Wu, and Mr. Ke Jiang for technical assistance in HRTEM, LLS, and FE-SEM experiments, respectively.

## References and Notes

- (1) Alivisatos, A. P. *Science* **1996**, 271, 933.
- (2) (a) Zhou, Y.; Yu, S. H.; Cui, X. P.; Wang, C. Y.; Chen, Z. Y. *Chem. Mater.* **1999**, 11, 545. (b) Zhu, J. J.; Liu, S. W.; Palchik, O.; Koltypin, Y.; Gedanken, A. *Langmuir* **2000**, 16, 6396. (c) Xu, D.; Xu, Y.; Chen, D.; Guo, G.; Gui, L.; Tang, Y. *Adv. Mater.* **2000**, 12, 520.
- (3) (a) Martin, C. R. *Science* **1994**, 226, 1961. (b) Huang, M. H.; Choudrey, A.; Yang, P. D. *Chem. Commun.* **2000**, 1063. (c) Tang, C.; Fan, S.; Lamy de la Chapelle, M.; Dang, H.; Li, P. *Adv. Mater.* **2000**, 12, 1346.
- (4) (a) Bhattacharya, S.; Saha, S. K.; Chakravorty, D. *Appl. Phys. Lett.* **2000**, 76, 3896. (b) Liu, S. W.; Yue, J.; Gedanken, A. *Adv. Mater.* **2001**, 13, 656. (c) Bhattacharya, S.; Saha, S. K.; Chakravorty, D. *Appl. Phys. Lett.* **2000**, 77, 3770. (d) Jana, N. R.; Gearheart, L.; Murphy, C. L. *Chem. Commun.* **2001**, 617.
- (5) (a) Morales, A. M.; Lieber, C. M. *Science* **1998**, 279, 208. (b) Gudiken, M. S.; Lieber, C. M. *J. Am. Chem. Soc.* **2000**, 122, 8801.
- (6) (a) Trentler, T. J.; Hickman, K. M.; Goel, S. C.; Viano, A. M.; Gibbons, P. C.; Buhro, W. E. *Science* **1995**, 270, 1791. (b) Gates, B.; Yin, Y.; Xia, Y. *J. Am. Chem. Soc.* **2000**, 122, 12582.
- (7) Wu, Y.; Yang, P. *Chem. Mater.* **2000**, 12, 605.
- (8) (a) Soullantica, K.; Maisonnat, A.; Senocq, F.; Fromen, M. C.; Casanove, M. J.; Chaudret, B. *Angew. Chem., Int. Ed.* **2001**, 40, 2984. (b) Yan, P.; Xie, Y.; Qian, Y.; Liu, X. *Chem. Commun.* **1999**, 1293.
- (9) Snoke, D. *Science* **1996**, 273, 1351.
- (10) (a) Switzer, J. A.; Manue, B. M.; Raub, E. R.; Bohannon, E. W. *J. Phys. Chem. B* **1999**, 103, 395. (b) Bohannon, E. W.; Huang, L. Y.; Miller, F. S.; Shumsky, M. G.; Switzer, J. A. *Langmuir* **1999**, 15, 813.
- (11) Kawanoe, H.; Yasukawa, M.; Hyodo, H.; Kurita, M.; Yanagi, H.; Hosono, H. *Nature* **1997**, 389, 939.
- (12) Poizot, P.; Laruelle, S.; Grugeon, S.; Dupont, L.; Taron, J. M. *Nature* **2000**, 407, 496.
- (13) (a) Huang, M. H.; Mao, S.; Feick, H.; Yan, H.; Wu, Y.; Kind, H.; Weber, E.; Russo, R.; Yang, P. *Science* **2001**, 292, 1897. (b) Hu, J. T.; Odom, T. W.; Lieber, C. M. *Acc. Chem. Res.* **1999**, 32, 435.
- (14) Singh, C. B.; Sahoo, B. *J. Inorg. Nucl. Chem.* **1974**, 36, 1259.
- (15) Bourrel, M.; Schechter, R. S. *Microemulsion and Related Systems: Formation, Solvency, and Physical Properties*; Marcel Dekker Inc.: New York, 1988; Surfactant Science Series Vol. 30.
- (16) Llanos, J.; Buljan, A.; Mujica, C.; Ramirez, R. *J. Alloys Compd.* **1996**, 234, 40.
- (17) Partain, L. D.; Schneider, R. A.; Donaghey, L. F.; Meleod, P. S. *J. Appl. Phys.* **1985**, 57, 5056.
- (18) Wanger, C. D.; Riggs, W. M.; Davis, L. E.; Moulder, J. F.; Muilenberg, G. E. *Handbook of X-ray Photoelectron Spectroscopy*; Perkin-Elmer Corp.: Eden Prairie, 1978.
- (19) Kazou, N. *Infrared and Raman Spectra of Inorganic and Coordination Compounds*; Wiley & Sons: New York, 1977.
- (20) Edwards, D. A.; Richards, R. *J. Chem. Soc., Dalton Trans.* **1975**, 639.
- (21) Berne, B. J.; Pecora, R. *Dynamic light scattering*; Academic Press: New York, 1976.
- (22) Chu, B. *Laser light scattering*, 2nd ed.; Academic Press: New York, 1991.
- (23) Stockmayer, W. H.; Schmid, M. *Pure Appl. Chem.* **1982**, 54, 407.
- (24) Appell, J.; Porte, G. *J. Colloid Interface Sci.* **1981**, 81, 85.